Physics Open 7 (2021) 100063

Contents lists available at ScienceDirect

Physics Open

journal homepage: www.journals.elsevier.com/physics-open

Smart magnetocaloric coatings for implants: Controlled drug release for targeted delivery

Aleksei S. Komlev, Radel R. Gimaev, Vladimir I. Zverev *

Faculty of Physics, M.V. Lomonosov Moscow State University, 119991, Moscow, Russia

ARTICLE INFO

Keywords:
Targeted drug delivery
Magnetocaloric effect
FeRh

ABSTRACT

Among the medical applications of the magnetocaloric effect (MCE) a technology of targeted drug delivery (TDD) is of great interest. The remote, noninvasive drug delivery to human organs or tissues is one of the actual challenges at present. Delivery devices, which provide a controlled, reproducible and reliable drug release, can have a significant impact on the treatment of different diseases. An ideal device for the fast drug delivery should contain a great amount of medication, should not practically release the drug in the off state, be able to repeatedly switch to the on state without mechanical damage, not require the implanted electronics, and be able to release a controlled dose of drug as stated in the physician's prescription.

This paper describes a composite material to coat implants and other drug carriers, which enables to control the quantity and the period of medication release. The paper also offers the results of thermodynamic model's analysis of these medical devices based on the properties of 'polymer/magnetic material' composite systems. The results of magnetic and nonmagnetic nanoparticles deposition on the fragments of abdominal meshes are also presented.

1. Introduction

Various types of endoprosthetics, such as vascular, esophageal, biliary and urinary duct surgery using stents, as well as joint prosthetics (joint replacement) are associated with the risks of infectious complications (occurring in 1–2% of cases), injuries caused by implants, as well as restenosis inside the stents (repeated vascular blockage, occurring in a significant number of cases (about 30%) within six to nine months after stent placement). Targeted delivery of bioactive substances (antibiotics, antiproliferative agents) is necessary to prevent such complications. In some cases the optimal therapeutic effect is achieved by periodically changing the concentration of bioactive substances in the tissues (pulsatile mode). The currently used methods of intravenous drug administration require much higher doses than in case of local exposure. Thus, it is necessary to develop implantable devices with improved properties capable of selectively affecting the affected tissues and releasing the drug in the right place in a controlled manner safely for the surrounding healthy tissues.

The surface of implants in contact with biological tissues must consist of biomedical material in order to improve tissue engraftment. Some implants have biological activity, such as subcutaneous drug dispensers in the form of implantable pills or drug-coated stents. Modern advances in implantation technology have led to significant advances in medicine, and the number of surgical procedures using implants is steadily increasing. Implants with magnetic elements are also beginning to play an increasing role in medicine. Examples of such magnetic implants are magnetic field concentrators for targeted drug delivery using intravenously injected magnetic nanoparticles, multifunctional ear implants on permanent magnets, etc. [1–4]. In addition, biodegradable devices with the functionality of reusable dispensers are also used in practice. For example, in Ref. [5] the device that consists of a biodegradable polymer microchip with microcontainers filled with various drugs is described. Another example [6] uses Peltier elements with a thermosensitive membrane that regulates the release of the drug in an aqueous environment. With such a device, a pulsating mode of drug release under the influence of electric current pulses has been realized. However, the implantation of chips, which are about a centimeter in size, limits the possible applications of such systems due to significant risks of trauma to healthy organs and tissues during their installation and extraction.

Targeted drug delivery using nanoparticles is the fastest growing area of nanotechnology applications in medicine. The most common approach to solving the problem of controlled drug release is the use of smart

* Corresponding author.
E-mail address: vi.zverev@physics.msu.ru (V.I. Zverev).

https://doi.org/10.1016/j.physo.2021.100063
Received 2 December 2020; Received in revised form 4 February 2021; Accepted 23 February 2021
Available online 27 February 2021

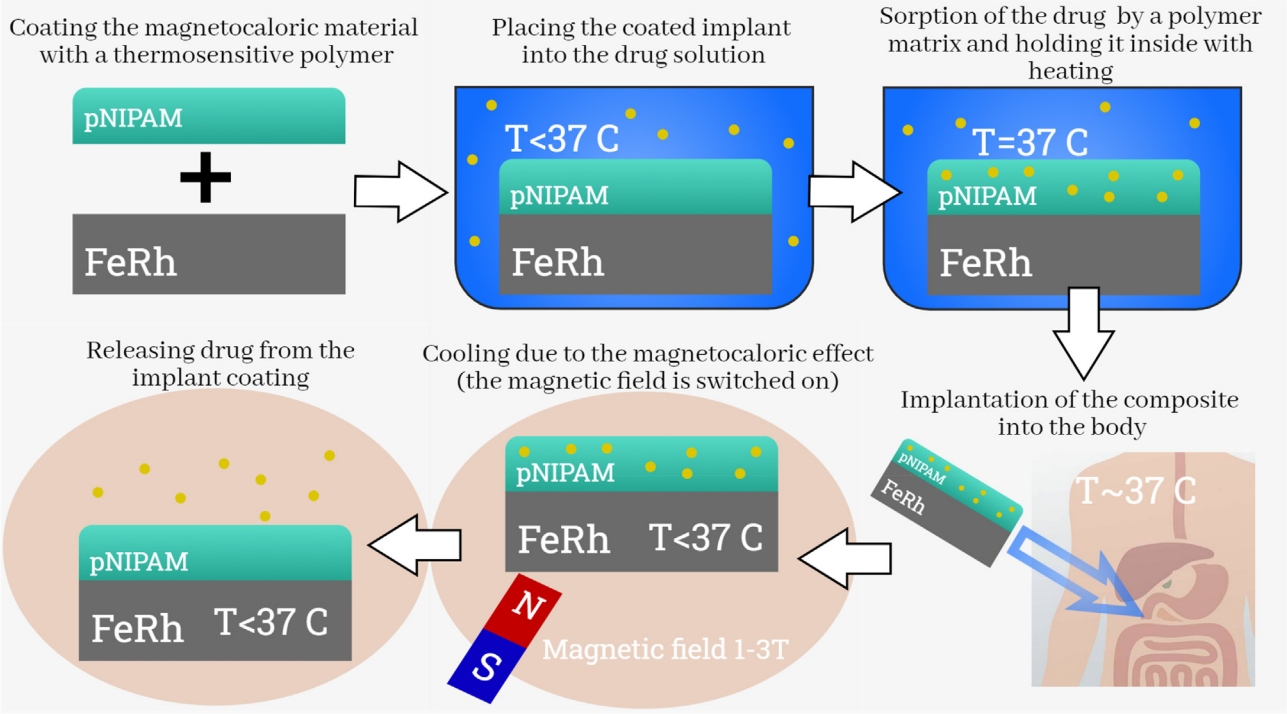

Fig. 1. The general mechanism of the drug release from the implant's surface.

polymers [7–10]. A more technological solution seems to be the coating of implants made of heat-sensitive polymers with nanoparticles heated by external influences, such as near-infrared radiation, which causes plasmon resonance in the nanoparticles of the coating [11]. However, biological tissues are not completely transparent even for infrared and microwave radiation, so the optimal way to externally control the condition of the implant coating seems to be exposure to a low-frequency or even constant magnetic field, which causes no side effects and, unlike constant electric field, infrared and microwave radiation, freely penetrates through biological tissues without weakening.

In [12] controlling the activity of a drug covering a metal implant (e.g., a stent) or a drug inside it is described. In this method, heating the stent allows releasing the drug from the coating layers, activating drug substances which biological activity is reduced or absent at body temperature, and increasing the interaction with the surrounding tissues at specified periods of time. Heat is supplied by exposing the stent with appropriate magnetic susceptibility to an electromagnetic field, preferably with a frequency lower than 1 MHz. The inductive heating is noninvasive and precisely controlled. However, heat release due to inductive heating is not easy to control because it depends on many parameters, including stent material and its position within the body. Consequently, there is an inherent risk of overheating the tissues surrounding the implant or not warming them sufficiently, which will reduce the effectiveness of the treatment. Due to the induction heating nature, only metallic materials can be used; accordingly, the use of biodegradable and plastic implants is excluded.

In [13] controlled embolization of an aneurysm is achieved using a magnetic field. The magnetic embolization system includes a catheter whose distal end is adapted to introduce a permanent magnet or electromagnet into a blood vessel aneurysm cavity, creating an internal magnetic field required for controlled embolization. However, insertion of such foreign and sufficiently large bodies creates great difficulties during surgeries.

Minor changes in the properties of the environment (pH factor, temperature, presence of certain substances, optical radiation, electric field) can lead to a change in the phase state of the polymer. The magnetic field does not affect the polymer directly, so it is resorted to an indirect effect: by heating the polymer containing magnetic nanoparticles in an alternating magnetic field [14], it is also possible to induce the magnetoelectric effect [15–17].

Examples of thermopolymer applications include poly-N-isopropylacrylamide (PNIPAm): an implantable Peltier element with a film containing a drug [6], and a composite membrane [14] with PNIPAm-based nanogel pores whose permeability depended on the membrane temperature, which was used for controlled drug release. It should be noted that either the thermoelectric effect [6] or nanoparticles remagnetization [14] are used for heating.

In the present work we have developed and described methods of applying functional coatings on implants, providing controlled release of bioactive substances by magnetic field in order to improve implant engraftment, prevent inflammatory processes, as well as restenosis inside the stent.

2. Conception

The composite coating consists of several components, the main of which are: magnetic material with a large magnetocaloric effect and thermosensitive polymer regulating the rate of drug (or other bioactive substance, for example, an antiproliferative agent) release. When a single exposure to a magnetic field of 1–3 T, the temperature change of the magnetocaloric material/polymer system should be about 2–7 °C, i.e. the biological tissue will cool to +32–35 °C, which excludes tissue necrosis, and is enough to change the polymer phase state and release the drug.

It is proposed to use FeRh as a magnetic material, which, like other alloys of iron with platinum group metals (e.g., FePt and FePd), has no toxic effect [18]; PNIPAm is supposed to be used as a polymer. The study of the biocompatibility of FeRh was not carried out in the present work. However, materials similar in their chemical and physical properties and also supposed to be used FePt and FePd are non-toxic, biocompatible and are widely used in the therapeutic practice of dental prosthetics [19,20]. The use of the FeRh alloy is preferable because it has a maximum magnetocaloric negative value, which increases the temperature range of the controlled release of the active ingredient.

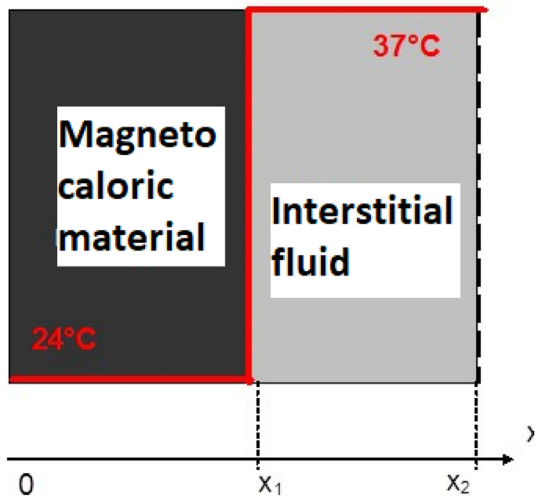

Fig. 2. The first stage of establishment of thermodynamic equilibrium in the system magnetic material-polymer-biological tissue.

The general mechanism of controlled release of bioactive substances from the decribed coating is presented in Fig. 1.

A general way to control the release of bioactive agents from the described coating has been previously described by the authors elsewhere [21,22].

PNIPAm is characterized by a lower critical dissolution temperature of +32 °C, which means that it is in a hydrophilic (swollen) state below +32 °C, and a hydrophobic (collapsed state) above this temperature. In the collapsed state, which corresponds to the temperature of the human body, the polymer retains the drug substances. The biocompatibility of PNIPAm has been proven *in vitro* [23] and *in vivo* [24], in both hydrophilic and hydrophobic phases. The proposed polymer is characterized by a reversible phase transition between two states: 'off', characterized by low diffusion rate of the drug substance, and 'on', with rapid drug release. Polymer glass transition or transition between swollen (highly soluble) and collapsed (hydrophobic) polymer states can be named as examples of such a phase transition. According to *in vitro* and *in vivo* studies, the use of such a polymer causes no adverse effects. The critical phase transition temperature is chosen close to the body temperature but not equal to it (in our case +32 °C) for the polymer to be in the collapsed state most of the time. As there is a certain difference in the temperature of different organs, endoprosthetics implies the use of polymers with somewhat different phase-transition temperatures in the range of +33–36°C. Tissue studies did not reveal any rejection or specific inflammation in response to the introduction of this material [25,26]. Preliminary experiments confirmed the possibility of fine-tuning the temperature of phase transitions of such polymers, as well as the discharge of active substances through the application of an external magnetic field. In this case, the bioactive substance is released by the polymer when the structural state of the polymer changes. In this case, a one-time 'salvo' release of the drug in case of urgent need can be carried out, among other things.

What distinguishes our conception from all previous studies is the idea of using the temperature decrease resulting from the giant magnetocaloric effect in FeRh (- 6K/T) [27–29], which allows to use the sharp phase transition (width ~1 °C) at +32 °C [6] in PNIPAm instead of the traditional heating used in magnetic therapy. Another characteristic feature of the magnetocaloric effect in FeRh is the narrow temperature range in which it occurs (due to the first order magnetic phase transition of the AFM-FM type observed in this alloy), which allows the treatment to be self-regulating in temperature [30], avoiding excessive temperature fluctuations (overcooling or overheating of the surrounding tissues), which can be caused by the magnetic field.

3. Thermodynamic model

In the present work we solved the problem of establishing thermodynamic equilibrium in a system of contacting metal layers and an interstitial fluid layer in which a hydrogel swells, bounded on both sides by thermal insulating layers, modeling a multilayer implant coating with a magnetocaloric layer and a thermosensitive polymer layer, surrounded by thermal insulating coatings from the implant and external environment [31].

According to the model, at the initial moment of time (Fig. 2) the magnetocaloric material is in the magnetic field and cooled to +24°C. The polymer is at body temperature +37°C.

The heat capacity of the system can be written as follows:

$$\frac{\partial \boldsymbol{U}}{\boldsymbol{dt}} = \frac{\boldsymbol{\kappa}}{\boldsymbol{C\rho}} \frac{\partial^2 \boldsymbol{U}}{\partial \boldsymbol{x}^2} \tag{1}$$

where $\boldsymbol{U}(\boldsymbol{x},\boldsymbol{t}) = \boldsymbol{T}(\boldsymbol{x},\boldsymbol{t}) - \boldsymbol{T}_0$ is a function of temperature equal to the difference between the current local temperature and the body temperature, $T_0 = 37°C$, κ is heat conductivity, C is heat capacity, ρ is density. Initial conditions are expressed as follows: $\boldsymbol{U}(\boldsymbol{x} < \boldsymbol{x}_1, 0) = \Delta \boldsymbol{T}$, $\boldsymbol{U}(\boldsymbol{x} > \boldsymbol{x}_1, 0) = 0$, where ΔT is the initial difference of temperatures.

The boundary conditions assume the absence of thermal conductivity at the boundaries of insulating layers: $\frac{\partial U(0,t)}{dx} = 0$, $\frac{\partial U(x_2,t)}{dx} = 0$.

The solution is sought in the form of a Fourier decomposition into spatial harmonics, q_n:

$$\boldsymbol{U} = \sum_{\boldsymbol{n}} \boldsymbol{A}_{\boldsymbol{n}} \cos(\boldsymbol{q}_{\boldsymbol{n}}\boldsymbol{x}) e^{-\frac{\kappa}{C\rho} q_n t} \tag{2}$$

Using the stitching condition of the solutions on the boundary $x = x_1$, one can obtain the characteristic equation:

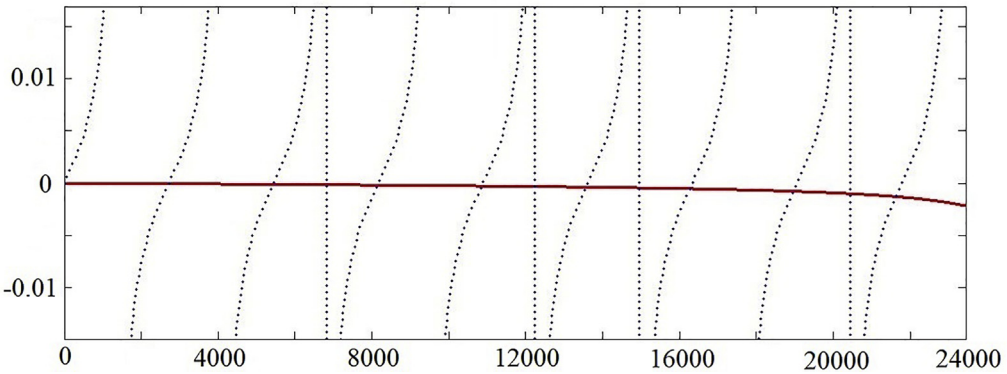

Fig. 3. Graphical solution for equation (5): the vertical axis are the values of the left and right parts of the equation, the horizontal axis are the values of q.

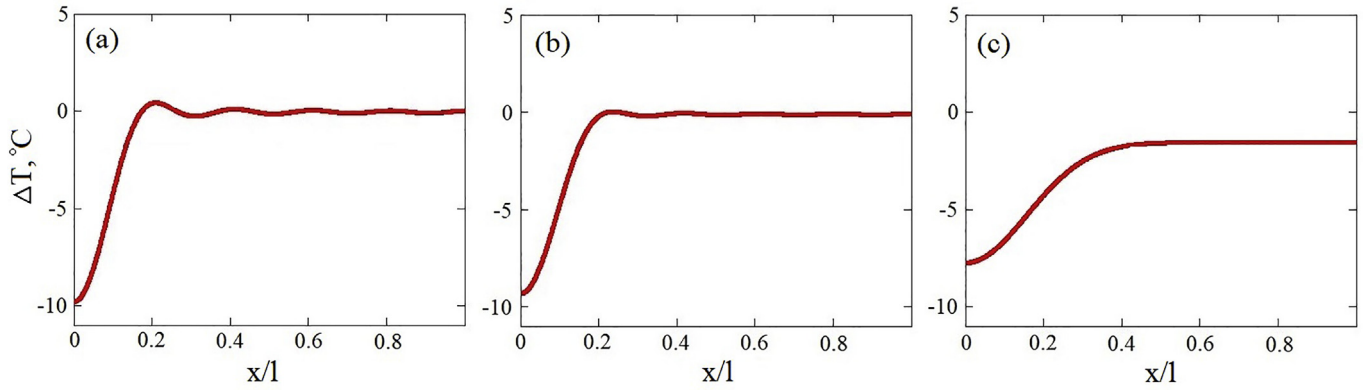

Fig. 4. Temperature distribution for three times: a) $0.001\tau_0$, b) $0.01\tau_0$, c)$0.1\tau_0$. The horizontal axis is the spatial coordinate of the cooled layer with polymer normalized to the layer thickness. The vertical axis is the temperature difference $U(x,t) = T(x,t) - T_0$ in degrees.

$$-\boldsymbol{q}_n^{(1)} \tan\left(\boldsymbol{q}_n^{(1)}\boldsymbol{x}_1\right) = \boldsymbol{q}_n^{(2)} \tan\left(\boldsymbol{q}_n^{(2)}(\boldsymbol{x}_2 - \boldsymbol{x}_1)\right) \tag{3}$$

Given that the stitching condition must be satisfied at any time, the condition for the interrelation of spatial frequencies is:

$$\frac{\boldsymbol{q}_n^{(1)}}{\boldsymbol{q}_n^{(2)}} = \sqrt{\frac{\boldsymbol{C}_1\boldsymbol{\rho}_1\boldsymbol{\kappa}_2}{\boldsymbol{C}_2\boldsymbol{\rho}_2\boldsymbol{\kappa}_1}} \tag{4}$$

Hence, a characteristic equation expressed through the layer parameters will be:

$$\tan(\boldsymbol{q}\boldsymbol{l}_1) = -\sqrt{\frac{\boldsymbol{C}_2\boldsymbol{\rho}_2\boldsymbol{\kappa}_1}{\boldsymbol{C}_1\boldsymbol{\rho}_1\boldsymbol{\kappa}_2}} \tan\left(\sqrt{\frac{\boldsymbol{C}_2\boldsymbol{\rho}_2\boldsymbol{\kappa}_1}{\boldsymbol{C}_1\boldsymbol{\rho}_1\boldsymbol{\kappa}_2}}\right)\boldsymbol{q}\boldsymbol{l}_2 \tag{5}$$

where q is the variable, l_1 and l_2 are the thicknesses of the layers of the magnetocaloric material and the polymer in the swollen state (in order for the polymer to remain in the swollen state, the temperature must be low in the entire layer), respectively.

Equation *(5)* is solved graphically (Fig. 3). The intersection points of the graphs give the spatial frequencies q_n in the expansion *(2)*.

Using the Fourier expansion for the initial temperature distribution one can obtain:

$$\boldsymbol{U}_1(\boldsymbol{x},\boldsymbol{t}) = \Delta\boldsymbol{T}_\infty + \frac{\Delta\boldsymbol{T}_0}{\boldsymbol{\pi}} \frac{\sin\left(\boldsymbol{q}_n^{(1)}\boldsymbol{l}_1\right)}{\boldsymbol{n}} \cos\left(\boldsymbol{q}_n^{(1)}\boldsymbol{x}\right) \boldsymbol{e}^{-\frac{\kappa_2}{C_2\rho_2}\boldsymbol{q}_n^2\boldsymbol{t}},\ \boldsymbol{x} \in (0,\boldsymbol{x}_1) \tag{6}$$

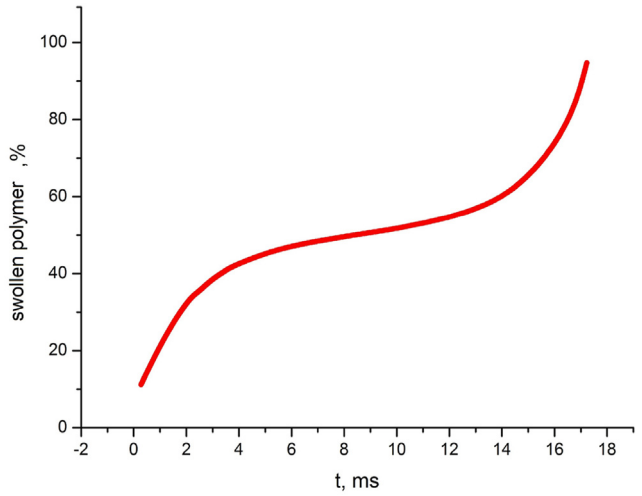

Fig. 5. Fraction of swollen polymer as a function of the pulse duration.

spin-lattice relaxation time ~100 ps, but much shorter than the swelling time of the polymer gel ~0.3 s.

Fig. 4 shows temperature dependencies at different moments of time in the considered area of the cooled layer, in which the polymer swells.

Since the temperature of the sections of the cooled layer located further from the magnetic layer decreases with a certain delay, by changing the duration of the magnetic pulse, it is possible to regulate which part of the layer cools down to the lower critical dissolution temperature and, accordingly, which part of the polymer swells up. The dependence of the polymer fraction that has undergone a phase transition on the pulse duration is presented in Fig. 5.

It should be noted that this dependence will appear more clearly the narrower the temperature interval in which the phase transition occurs. At a transition width of the order of one degree, the phase transition in the entire volume already occurs in time $\sim\tau_0$. Finally, at the final stage of the phase transition, polymer swells and drug release occurs. Both processes have a diffusion character, i.e., their characteristic time scales

$$\boldsymbol{U}_2(\boldsymbol{x},\boldsymbol{t}) = \Delta\boldsymbol{T}_\infty\left(1 - \boldsymbol{e}^{-\frac{\kappa_2}{C_2\rho_2}\boldsymbol{q}_n^2\boldsymbol{t}}\right) + + \frac{\Delta\boldsymbol{T}_0}{\boldsymbol{\pi}} \sum \frac{\sin\left(\boldsymbol{q}_n^{(2)}\boldsymbol{l}_2\right)\cos\left(\boldsymbol{q}_n^{(2)}\boldsymbol{l}_2\right)\left(\cos\left(\boldsymbol{q}_n^{(2)}\boldsymbol{x}\right) + \sin\left(\boldsymbol{q}_n^{(2)}\boldsymbol{x}\right)\tan\left(\boldsymbol{q}_n^{(2)}\boldsymbol{l}_2\right)\right)}{\cos\left(\boldsymbol{q}_n^{(2)}\boldsymbol{l}_2\right) + \sin\left(\boldsymbol{q}_n^{(2)}\boldsymbol{l}_2\right)\tan\left(\boldsymbol{q}_n^{(2)}\boldsymbol{l}_2\right)} \boldsymbol{e}^{-\frac{\kappa_2}{C_2\rho_2}\boldsymbol{q}_n^2\boldsymbol{t}},\ \boldsymbol{x} \in (\boldsymbol{x}_1,\boldsymbol{x}_2), \tag{7}$$

where $\Delta T_\infty = \frac{C_1\rho_1 l_1 \Delta T_0}{C_1\rho_1 l_1 + C_2\rho_2 l_2}$ is a final temperature after the establishment of thermodynamic equilibrium. The characteristic time of establishment of thermodynamic equilibrium can also be determined as $\tau_0 = \frac{C\rho}{\kappa q_1}$.

For the chosen parameters of FeRh: thermal conductivity 150 W/m K, heat capacity C = 300 J/(kg·K), density, ρ = 10 g/cm^3, a layer width l_1 = 60 μm and hydrogel PNIPAm of the same thickness with thermal conductivity 0.56 W/m K, heat capacity C = 4200 J/(kg K), ρ = 1 g/cm^3 at initial temperature difference of - 13 °C (which is achievable in 2T magnetic field) the thermodynamic equilibrium temperature is equal $\Delta T_\infty = +32$°C, which corresponds to polymer phase transition temperature (lower critical dissolution temperature). In this case, the characteristic time of equilibration is about 1 ms, which is much longer than the

according to the law $\tau \sim l^2$, where l is a characteristic dimension.

Using experimental data for collapse time with 100 nm diameter particles (characteristic size of microstructure is l_1) equal to 360 ns [7], from $\frac{\tau_2}{\tau_1} = \frac{l_2^2}{l_1^2} = 10^6$ one can evaluate the characteristic time for the phase transition into the hydrophobic-hydrophilic state for the 100 μm (l_2) layer as 0.3 s. By varying the duration of the magnetic pulse, it is possible to change the polymer fraction that has undergone a phase transition, which allows to dose the amount of the released drug. The problem then is reduced to determining what concentration of the drug was contained in this polymer (variation initial condition which is determined by the type of the medicine, its concentration etc) [32].

4. Experiment

In this work a magnetically controlled implantable device was tested to verify its ability to encapsulate and release the active substance when a magnetic field is applied. A prototype of the implantable device was made by deposition of a 0.1 mm thick gadolinium film on a polystyrene plate. Gd has a positive magnetocaloric effect of about 3 K/T at 294 K [33]. Then a PNIPAm polymer film with a thickness of 10 μm was created on Gd foil by casting method. The resulting composite structure was placed in a solution of colchicine with a concentration of 1 mg/cm^3 with a temperature +25 °C, below the lower critical dissolution temperature of PNIPAm (+32 °C). The polymer film was in a swollen hydrophilic state with a thickness of 100 μm, allowing it to be loaded with colchicine. The composite structure was then washed with hot water (at a temperature above the lower critical dissolution temperature), which caused the collapse of the polymer and trapping the drug in its volume, while no colchicine remained on the surface. The amount of colchicine per 1 cm^2 of the surface was 0.1 μg. Finally, the polymer was covered with a layer of mesoporous ZrO2 bioceramics, resulting in a sandwich structure with a composite of layers of heat-sensitive polymer and magnetocaloric material sandwiched between two heat-insulating layers. Further, the prototype described above and the NCTC clone L929 cell line were used in the cytotoxic test. A solution containing the culture maintained at +37 °C was placed in a 10 ml tube. The prototype device was immersed in the solution. Then, slowly (so that the process proceeded isothermally and the heat released in Gd due to MCE would have time to dissipate) a permanent magnet was brought up, thus gradually increasing the field in the test tube to 2 T at a constant solution temperature of +37 °C. Then the magnet was abruptly removed, causing the temperature to drop to +32 °C due to MCE and the release of colchicine. The solution was then incubated at +37 °C for 24 h. The number of live and dead cells was then counted by microscope observation in a Goryaev chamber using Syto9 and propidium iodide dyes. The Syto9 dye penetrates the membranes of living and dead cells, staining DNA and RNA green (video in Supplement materials demonstrates the experiment with dye release in a magnetic field). Propidium iodide penetrates the membranes of dead cells only, staining the nuclei red. This makes dead and living cells visible for counting in the microscope. In this experiment, only 10% of the cells survived after 24 h. In the case of direct addition of colchicine with a concentration of 0.1 μg/cm^3 to the solution, 99% of the bacteria survived. Such a significant difference in cytotoxicity can be explained by the adsorption of cells on the surface of the implant prototype, near which the concentration of colchicine is increased due to its release from the polymer layer. This circumstance is an advantage because in most cases complications develop in the area adjacent to the implant surface, and it is in this area that there should be an increased concentration of the drug. At the same time, intravenous injection is similar to the direct injection of colchicine in solution in the experiment, which leads to low drug concentration near the implant surface and to the development of side effects in healthy tissues.

The same test protocol was followed for the $Fe_{0,49}Rh_{0,51}$ foil. FeRh exhibits a negative magnetocaloric effect of −6 K/T at 232 K [34]. Accordingly, the cooling required for colchicine resetting was carried out by fast bringing a permanent magnet to the tube with the drug, thus providing a rapid change in the magnetic field from zero to 2 T and cooling of the sample. Once thermodynamic equilibrium was established at +37 °C, the magnet was slowly removed from the tube. The temperature +37 °C was maintained using a thermostat for 24 h. After this timel, the number of live and dead cells was estimated. In this case, 3% of live cells remained after 24 h.

Several tests have been carried out on abdominal meshes (mesh-type implants used in surgery) coated with the polymer-magnetic material composite. The polypropylene abdominal meshes were coated with the magnetic nanoparticles (magnetite Fe_3O_4) and tungsten nanoparticles using the layer-by-layer deposition.

An original method of layer-by-layer deposition of nanoparticles on a polymer coating of polypropylene and polyvinyl difluoride was developed to coat abdominal meshes with nanoparticles (Fig. 6). The layer-by-layer deposition technique is based on the electrostatic attraction of oppositely charged layers applied in series.

Step 1 A gel layer of positively charged polyelectrolyte, polyallylamine hydrochloride, is applied to the polypropylene and polyvinyl difluoride surface to be coated with the functional coating.
Step 2 The surface is washed with distilled water.
Step 3 Negatively charged nanoparticles are deposited on the surface.
Step 4 The surface is washed with distilled water.

Then the process is cyclically repeated in the number of cycles equal to the required number of layers (one can try different amount of layers to study the dependence of the substance release on this matter). After application the surface is dried.

In vitro studies were performed on the abdominal mesh fragments: in a 7 T field from ClinScan MRI (Bruker BioSpin), tubes with physiological solution containing samples with magnetic nanoparticles and with tungsten particles were repeatedly inserted and withdrawn (Fig. 7). After exposure to the magnetic field and exposure of the samples, not only the magnetic coating of nanoparticles was observed to decay, but also the grid structure itself was destroyed (Fig. 7b and c).

Immediately after exposure to the field from MRI, only a slight release from the mesh coating with magnetic nanoparticles under the influence of the magnetic field was observed (Fig. 8a). While the greatest release of particles from the mesh surface was observed for tungsten nanoparticles, which took place even in the absence of the magnetic field, which is

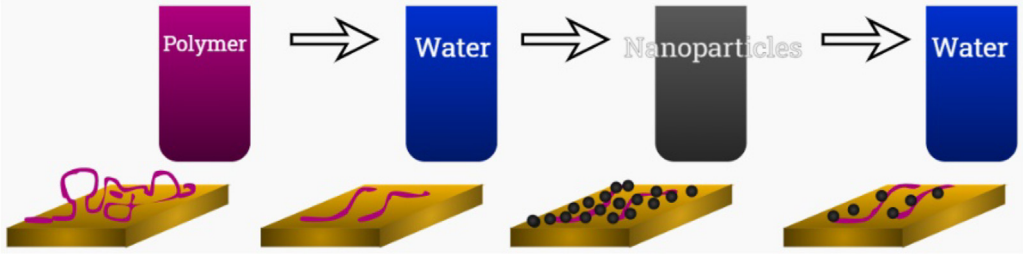

Fig. 6. Layer-by-layer deposition method.

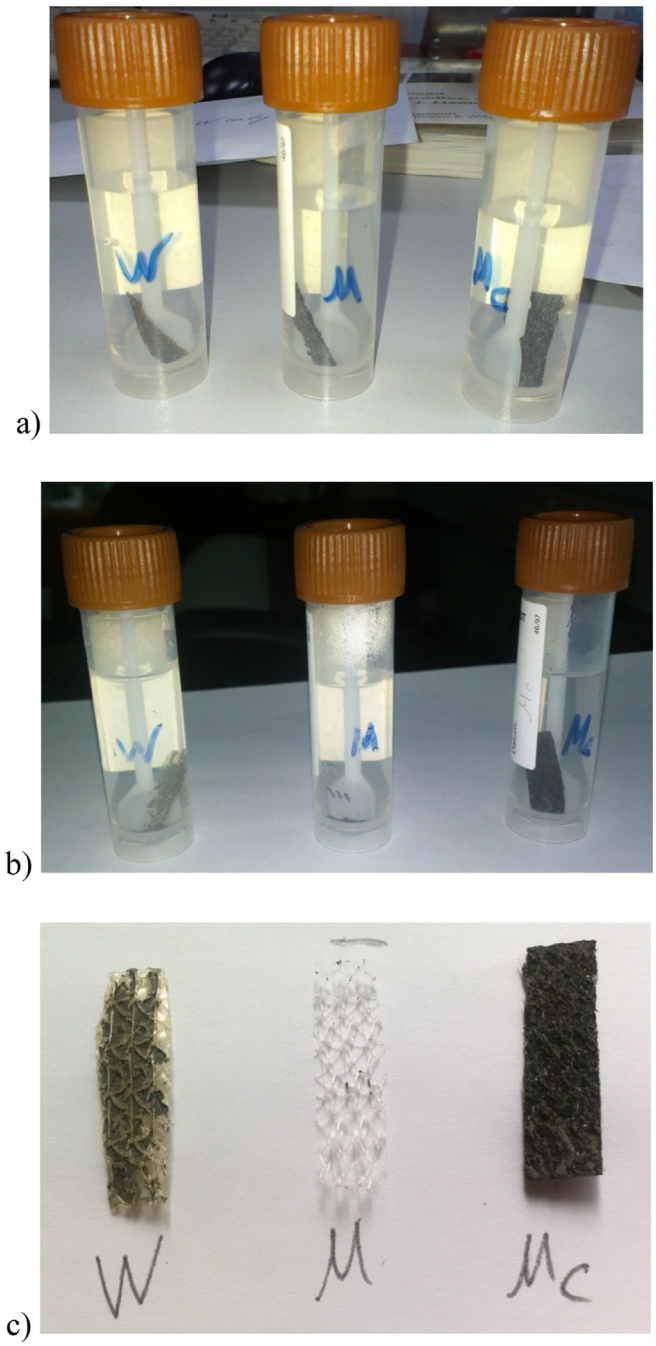

Fig. 7. Fragments of abdominal meshes in physiological solution: a) before the experiment (left tube with a fragment of the mesh with applied tungsten particles, central and right - with applied magnetic nanoparticles; b) condition of samples after repeated placement of two tubes in the MRI field and a week exposure (extreme-right tube - control, it remained outside the field): grid with magnetic particles, which has been in MRI (the central tube) practically remained without a coating of nanoparticles; c) the same grids after drying: the destruction of the central grid structure is clearly visible.

explained by the weak adhesion of the particles on the surface of polypropylene. The convergence of the mesh coating with magnetic nanoparticles in saline solution in the absence of a magnetic field was insignificant, which suggests its stability on the implant surface (Fig. 8).

After prolonged (more than a week) exposure of the samples in saline, the picture changed dramatically: the greatest convergence of coverage was observed for the mesh with magnetic nanoparticles exposed to the MRI field, while the appearance of the mesh with tungsten particles and

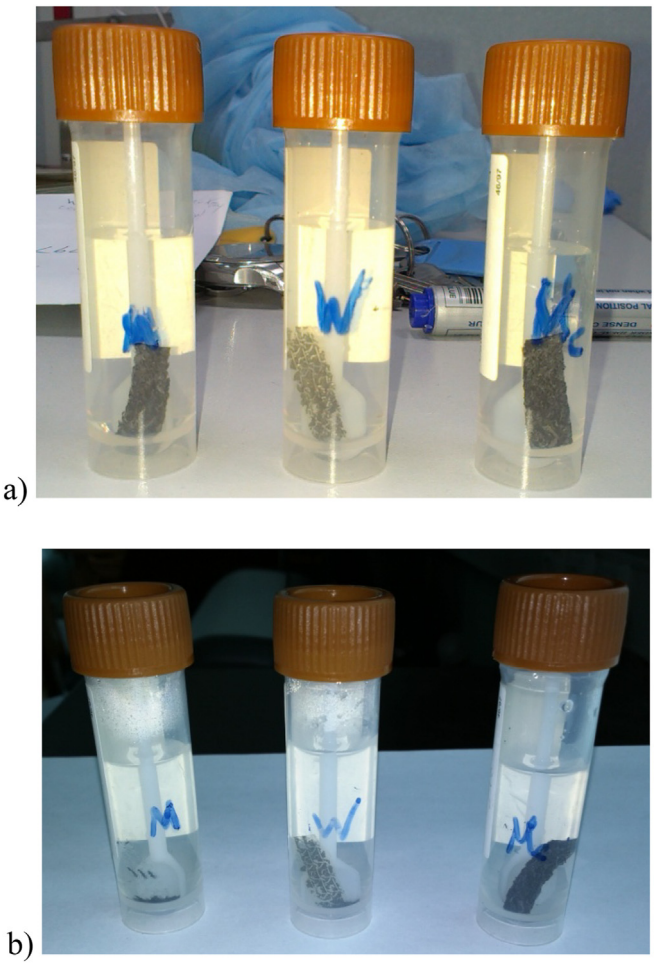

Fig. 8. Dynamics of the coating removal: a) the view of the meshes immediately after exposure to the magnetic field; b) the view after 3 weeks of exposure. From left to right: mesh with magnetic nanoparticles exposed to magnetic field, in the center - mesh with tungsten nanoparticles, on the right - mesh with magnetic nanoparticles, not exposed to the field from MRI.

the mesh with magnetic particles that were not exposed to MRI changed insignificantly (Fig. 8b). Thus, the release of 90%–100% of magnetic nanoparticles exposed to the magnetic field is observed on long time intervals.

Agglomerates of nanoparticles emitted from the meshes are clearly seen (Fig. 9).

Gd and W here act as model objects, on which the claimed effects are well demonstrated, in particular, the significant magnetocaloric effect in gadolinium (a giant magnetocaloric response when the magnetic field is switched on), and the X-ray contrasting in the example of tungsten nanoparticles. The problem of toxicity of certain materials in the form of nanoparticles is now quite easily solved by applying appropriate coatings, a number of articles on the subject added to the list of references [35–38].

The described effect may be of interest for therapy using prolonged-acting drugs with the possibility of externally triggering the drug release process. By varying the particle size and the number of layers, a given drug concentration and drug release rate can be achieved.

5. Conclusions

Thus, the ‘smart coating’ of the implant developed in this work is characterized by the following functions:

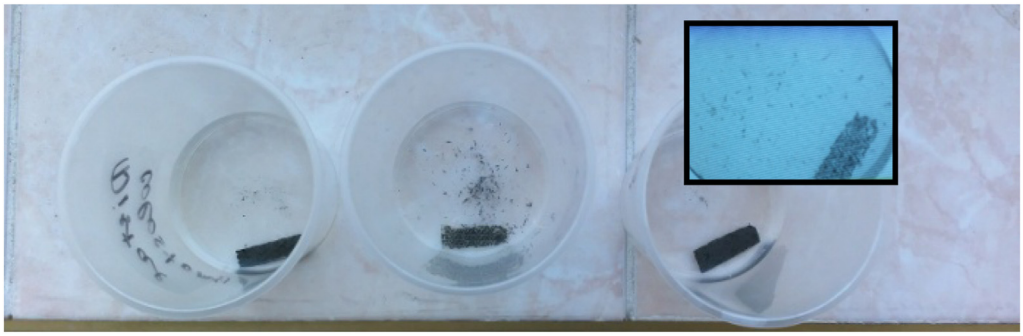

Fig. 9. Fragments of the same meshes right after exposure to the magnetic field, top view. The inset shows an X-ray image.

- Preservation of the drug in the implant shell and its release at the right moment of time at the implant location;
- Non-invasive and remote control of the coating state (by applying an external magnetic field), which provides regulated mode of bioactive substance release (including drug release in pulsating mode) due to temperature change of the magnetic coating component and induced change of the phase state of the polymer containing the drug. It is assumed that control of the coating state is performed by measuring the magnitude of the external magnetic field and the time elapsed since its application. Control of the phase transition dynamics will also allow controlling the process of substance release to a great extent.
- self-regulated temperature regime (without the use of invasive temperature sensors), by selecting the temperature of magnetic phase transition near the human's body temperature;
- the principal possibility to replenish the bioactive substance in the implant coating.

The technology can be used in different fields of medicine, respectively, the type of implant and substance applied to it will vary depending on the disease [for example, in case of urolithiasis, ureteral narrowings, any external compression (including stent placement) leads to formation of scar tissue; by introducing drugs that prevent fermentation (heparin, etc.) into the coating of the ureteral stent, it is possible to prevent scarring; by introducing drugs that prevent fermentation (heparin, etc.) into the ureteral stent. It is possible to prevent scarring; in the case of hip replacement surgery (it is located in the area of the passage of the great vessels, so this operation is accompanied by heavy bleeding, which increases the risk of infection) the endoprosthesis can be coated with an embedded antibiotic that prevents suppuration (amosiclave, flemoxin, etc.)].

Thus, the described studies provide a basis for an analog of the magnetocaloric magnetoplastic material to be used in the targeted drug delivery. This structure is submicron particles of the FeRh alloy, which undergo the phase transition in the region of the human body temperature and reveal the noticeable magnetocaloric properties in the powder form placed in the polymer matrix with the drug.

Data availability

The data that support the findings of this study are available from the corresponding author upon reasonable request.

CRediT authorship contribution statement

Aleksei S. Komlev: Software, Data curation. **Radel R. Gimaev:** Software, Data curation, Investigation. **Vladimir I. Zverev:** Conceptualization, Methodology, Writing – original draft.

Declaration of competing interest

The authors declare that they have no known competing financial interests or personal relationships that could have appeared to influence the work reported in this paper.

Acknowledgements

The authors are thankful to Prof. Alexander P. Oettinger, M.D. (Pirogov Russian National Research Medical University), Prof. Iouri Gounko (Trinity College Dublin) and Prof. Alexander P. Pyatalov (Moscow State University) for useful discussions and the help in experiments. Komlev A.S. is a fellow of the Theoretical Physics and Mathematics Advancement Foundation "BASIS".

References

[1] Z.G. Forbes, B.B. Yellen, D.S. Halverson, G. Fridman, K.A. Barbee, G. Friedman, Validation of high gradient magnetic field based drug delivery to magnetizable implants under flow, IEEE (Inst. Electr. Electron. Eng.) Trans. Biomed. Eng. 55 (2008) 643–649, https://doi.org/10.1109/TBME.2007.899347.

[2] T.N. Le, L. Straatman, A. Yanai, R. Rahmanian, C. Garnis, U.O. Häfeli, T. Poblete, B.D. Westerberg, K. Gregory-Evans, Magnetic stem cell targeting to the inner ear, J. Magn. Magn Mater. 443 (2017) 385–396, https://doi.org/10.1016/j.jmmm.2017.07.033.

[3] S. Mondal, P. Manivasagan, S. Bharathiraja, M. Santha Moorthy, H.H. Kim, H. Seo, K.D. Lee, J. Oh, Magnetic hydroxyapatite: a promising multifunctional platform for nanomedicine application, Int. J. Nanomed. 12 (2017) 8389–8410, https://doi.org/10.2147/IJN.S147355.

[4] P.M. Price, W.E. Mahmoud, A.A. Al-Ghamdi, L.M. Bronstein, Magnetic drug delivery: where the field is going, Front. Chem. 6 (2018), https://doi.org/10.3389/fchem.2018.00619.

[5] A.C.R. Grayson, I.S. Choi, B.M. Tyler, P.P. Wang, H. Brem, M.J. Cima, R. Langer, Multi-pulse drug delivery from a resorbable polymeric microchip device, Nat. Mater. 2 (2003) 767–772, https://doi.org/10.1038/nmat998.

[6] R. Yang, A.V. Gorelov, F. Aldabbagh, W.M. Carroll, Y. Rochev, An implantable thermoresponsive drug delivery system based on Peltier device, Int. J. Pharm. 447 (2013) 109–114, https://doi.org/10.1016/j.ijpharm.2013.02.051.

[7] Z. Ahmed, E.A. Gooding, K.V. Pimenov, L. Wang, S.A. Asher, UV resonance Raman determination of molecular mechanism of poly(N-isopropylacrylamide) volume phase transition, J. Phys. Chem. B 113 (2009) 4248–4256, https://doi.org/10.1021/jp810685g.

[8] C. de las H. Alarcón, S. Pennadam, C. Alexander, Stimuli responsive polymers for biomedical applications, Chem. Soc. Rev. 34 (2005) 276–285, https://doi.org/10.1039/B406727D.

[9] I.Y. Galaev, "Smart" polymers in biotechnology and medicine, Russ. Chem. Rev. 64 (1995) 471, https://doi.org/10.1070/RC1995v064n05ABEH000161.

[10] T.T.N. Vo, R. Yang, F. Aldabbagh, W. Carroll, M. Meere, Y. Rochev, A thermally activated drug delivery system based on a thermoresponsive polymer and a cooling device: a theoretical assessment, J. Therm. Sci. Eng. Appl. 6 (2014), https://doi.org/10.1115/1.4025935.

[11] S.R. Sershen, S.L. Westcott, N.J. Halas, J.L. West, Temperature-sensitive polymer–nanoshell composites for photothermally modulated drug delivery, J. Biomed. Mater. Res. 51 (2000) 293–298, https://doi.org/10.1002/1097-4636(20000905)51:3<293::AID-JBM1>3.0.CO;2-T.

[12] W. Daum, M.L.B. Anderson, R.A. Mazzicchi, Stent and Method for Drug Delivery from Stents, US20020128704A1, 2005. https://patents.google.com/patent/US6935121B2/en. (Accessed 23 October 2018).

[13] M.P. Wallace, J.C. Eder, C. Teoh, Apparatus and Method for Controlling a Magnetically Controllable Embolic in the Embolization of an Aneurysm, US6544163B2, 2003. https://patents.google.com/patent/US6544163B2/en?oq=US+6544163. (Accessed 27 April 2020).
[14] T. Hoare, J. Santamaria, G.F. Goya, S. Irusta, D. Lin, S. Lau, R. Padera, R. Langer, D.S. Kohane, A magnetically triggered composite membrane for on-demand drug delivery, Nano Lett. 9 (2009) 3651–3657, https://doi.org/10.1021/nl9018935.
[15] R. Guduru, P. Liang, C. Runowicz, M. Nair, V. Atluri, S. Khizroev, Magneto-electric nanoparticles to enable field-controlled high-specificity drug delivery to eradicate ovarian cancer cells, Sci. Rep. 3 (2013) 1–8, https://doi.org/10.1038/srep02953.
[16] M. Nair, R. Guduru, P. Liang, J. Hong, V. Sagar, S. Khizroev, Externally controlled on-demand release of anti-HIV drug using magneto-electric nanoparticles as carriers, Nat. Commun. 4 (2013) 1–8, https://doi.org/10.1038/ncomms2717.
[17] K. Yue, R. Guduru, J. Hong, P. Liang, M. Nair, S. Khizroev, Magneto-electric nanoparticles for non-invasive brain stimulation, PloS One 7 (2012), e44040, https://doi.org/10.1371/journal.pone.0044040.
[18] R.R. Gimaev, A.A. Vaulin, A.F. Gubkin, V.I. Zverev, Peculiarities of magnetic and magnetocaloric properties of Fe–Rh alloys in the range of antiferromagnet–ferromagnet transition, Phys. Met. Metallogr. 121 (2020) 823–850, https://doi.org/10.1134/S0031918X20090045.
[19] Y. Tanaka, K. Hisatsune, Remanence enhancement based on L10 ordering in Fe–Pt permanent magnets, J. Appl. Phys. 93 (2003) 3435–3439, https://doi.org/10.1063/1.1555675.
[20] A. Gebert, S. Roth, R. Gopalan, A.A. Kündig, L. Schultz, Corrosion behaviour of FePt-based bulk magnets in artificial saliva solution, J. Alloys Compd. 436 (2007) 309–312, https://doi.org/10.1016/j.jallcom.2006.07.016.
[21] A.M. Tishin, Y.I. Spichkin, V.I. Zverev, P.W. Egolf, A review and new perspectives for the magnetocaloric effect: new materials and local heating and cooling inside the human body, Int. J. Refrig. 68 (2016) 177–186, https://doi.org/10.1016/j.ijrefrig.2016.04.020.
[22] A.M. Tishin, J.A. Rochev, A.V. Gorelov, Magnetic Carrier and Medical Preparation for Controllable Delivery and Release of Active Substances, Methods of Their Production and Methods of Treatment Using Thereof, US9017713B2, 2015. https://patents.google.com/patent/US9017713B2/en?oq=US9017713+B2+. (Accessed 2 May 2020).
[23] T. Takezawa, Y. Mori, K. Yoshizato, Cell culture on a thermo-responsive polymer surface, Nat. Biotechnol. 8 (1990) 854–856.
[24] H. Malonne, F. Eeckman, D. Fontaine, A. Otto, L. De Vos, A. Moës, J. Fontaine, K. Amighi, Preparation of poly(N-isopropylacrylamide) copolymers and preliminary assessment of their acute and subacute toxicity in mice, Eur. J. Pharm. Biopharm. 61 (2005) 188–194, https://doi.org/10.1016/j.ejpb.2005.05.007.
[25] V. Capella, R.E. Rivero, A.C. Liaudat, L.E. Ibarra, D.A. Roma, F. Alustiza, F. Mañas, C.A. Barbero, P. Bosch, C.R. Rivarola, N. Rodriguez, Cytotoxicity and bioadhesive properties of poly-N-isopropylacrylamide hydrogel, Heliyon 5 (2019), e01474, https://doi.org/10.1016/j.heliyon.2019.e01474.
[26] Z. Guo, S. Li, C. Wang, J. Xu, B. Kirk, J. Wu, Z. Liu, W. Xue, Biocompatibility and cellular uptake mechanisms of poly(N-isopropylacrylamide) in different cells, J. Bioact. Compat Polym. 32 (2017) 17–31, https://doi.org/10.1177/0883911516648969.
[27] V.I. Zverev, A.M. Saletsky, R.R. Gimaev, A.M. Tishin, T. Miyanaga, J.B. Staunton, Influence of structural defects on the magnetocaloric effect in the vicinity of the first order magnetic transition in Fe50.4Rh49.6, Appl. Phys. Lett. 108 (2016) 192405, https://doi.org/10.1063/1.4949355.
[28] C.F. Sánchez-Valdés, R.R. Gimaev, M. López-Cruz, J.L. Sánchez Llamazares, V.I. Zverev, A.M. Tishin, A.M.G. Carvalho, D.J.M. Aguiar, Y. Mudryk, V.K. Pecharsky, The effect of cooling rate on magnetothermal properties of Fe49Rh51, J. Magn. Magn Mater. 498 (2020) 166130, https://doi.org/10.1016/j.jmmm.2019.166130.
[29] A. Chirkova, K.P. Skokov, L. Schultz, N.V. Baranov, O. Gutfleisch, T.G. Woodcock, Giant adiabatic temperature change in FeRh alloys evidenced by direct measurements under cyclic conditions, Acta Mater. 106 (2016) 15–21, https://doi.org/10.1016/j.actamat.2015.11.054.
[30] V.I. Zverev, A.M. Tishin, M.D. Kuz'min, The maximum possible magnetocaloric ΔT effect, J. Appl. Phys. 107 (2010), 043907, https://doi.org/10.1063/1.3309769.
[31] V.I. Zverev, A.P. Pyatakov, A.A. Shtil, A.M. Tishin, Novel applications of magnetic materials and technologies for medicine, J. Magn. Magn. Mater. 459 (1 August 2018) 182–186, https://doi.org/10.1016/j.jmmm.2017.11.032.
[32] Y.I. Spichkin, A.P. Pyatakov, A.M. Tishin, V.I. Zverev, A Magnetic Field Controllable Implantable Device and a Method of Controlled Drug Release Therefrom, GB2520960A, 2015. https://patents.google.com/patent/GB2520960A/en?oq=GB2520960. (Accessed 17 July 2020).
[33] S.Yu Dan'kov, A.M. Tishin, V.K. Pecharsky, K.A. Gschneidner, Magnetic phase transitions and the magnetothermal properties of gadolinium, Phys. Rev. B 57 (1998) 3478–3490, https://doi.org/10.1103/PhysRevB.57.3478.
[34] S.A. Nikitin, G. Myalikgulyev, A.M. Tishin, M.P. Annaorazov, K.A. Asatryan, A.L. Tyurin, The magnetocaloric effect in Fe49Rh51 compound, Phys. Lett. 148 (1990) 363–366, https://doi.org/10.1016/0375-9601(90)90819-A.
[35] D.V. Quy, N.M. Hieu, P.T. Tra, N.H. Nam, N.H. Hai, N. Thai Son, P.T. Nghia, N.T.V. Anh, T.T. Hong, N.H. Luong, Synthesis of silica-coated magnetic nanoparticles and application in the detection of pathogenic viruses, J. Nanomater. 2013 (2013), e603940, https://doi.org/10.1155/2013/603940.
[36] D.-W. Lee, H. Fatima, K.-S. Kim, Preparation of silica coated magnetic nanoparticles for bioseparation, J. Nanosci. Nanotechnol. 18 (2018) 1414–1418, https://doi.org/10.1166/jnn.2018.14888.
[37] S.M. Silva, R. Tavallaie, L. Sandiford, R.D. Tilley, J.J. Gooding, Gold coated magnetic nanoparticles: from preparation to surface modification for analytical and biomedical applications, Chem. Commun. 52 (2016) 7528–7540, https://doi.org/10.1039/C6CC03225G.
[38] L. León Félix, B. Sanz, V. Sebastián, T.E. Torres, M.H. Sousa, J.a.H. Coaquira, M.R. Ibarra, G.F. Goya, Gold-decorated magnetic nanoparticles design for hyperthermia applications and as a potential platform for their surface-functionalization, Sci. Rep. 9 (2019) 4185, https://doi.org/10.1038/s41598-019-40769-2.